

## 1 2      **Unsuspected involvement of spinal cord in Alzheimer Disease.** 3

4      **Roberta Maria Lorenzi**<sup>1\*</sup>, **Fulvia Palesi**<sup>2,3</sup>, **Gloria Castellazzi**<sup>1,4</sup>, **Paolo Vitali**<sup>3</sup>, **Nicoletta Anzalone**<sup>5</sup>,  
5      **Sara Bernini**<sup>6</sup>, **Elena Sinforiani**<sup>6</sup>, **Giuseppe Micieli**<sup>7</sup>, **Alfredo Costa**<sup>2,8</sup>, **Egidio D'Angelo**<sup>2,9</sup>, and **Claudia**  
6      **A.M. Gandini Wheeler-Kingshott**<sup>4,2,10</sup>

7      1Department of Electrical, Computer and Biomedical Engineering, University of Pavia, Pavia, Italy,

8      2Department of Brain and Behavioral Sciences, University of Pavia, Pavia, Italy,

9      3Neuroradiology Unit, Brain MRI 3T Research Center, IRCCS Mondino Foundation, Pavia, Italy,

10      4Queen Square MS Centre, Department of Neuroinflammation, UCL Queen Square Institute of Neurology,

11      Faculty of Brain Sciences, University College London, London, United Kingdom,

12      5Universita Vita e Salute, S Raffaele hospital Milan

13      6Laboratory of Neuropsychology, IRCCS Mondino Foundation, Pavia, Italy,

14      7Department of Emergency Neurology, IRCCS Mondino Foundation, Pavia, Italy,

15      8Unit of Behavioral Neurology, IRCCS Mondino Foundation, Pavia, Italy,

16      9Brain connectivity center (BCC), IRCCS Mondino Foundation, Pavia, Italy,

17      10Brain MRI 3T Research Center, IRCCS Mondino Foundation, Pavia, Italy

18      **\*Correspondence:**

19      Dr.ssa Roberta Maria Lorenzi

20      robertamaria.lorenzi01@universitadipavia.it

21      **Keywords: Dementia - Alzheimer disease, cross sectional area (CSA), brain atrophy, Spinal**  
22      **cord atrophy, Spinal Cord Toolbox, Alzheimer diagnosis, Dementia biomarker, Sensorymotor**  
23      **function impairment.**

24      **Number of words (Introduction, Material and Methods, Results, Discussion): 3660**

25      **Number of Figures: 4**

26      **Abstract**

27      **Objective:** Brain atrophy is an established biomarker for dementia, yet spinal cord involvement has  
28      not been investigated to date. As the spinal cord is relaying sensorimotor control signals from the  
29      cortex to the peripheral nervous system and viceversa, it is indeed a very interesting question to  
30      assess whether it is affected by atrophy in a disease that is known for its involvement of cognitive  
31      domains first and foremost, with motor symptoms being clinically assessed too. We therefore  
32      hypothesize that Alzheimer Disease severe atrophy can affect the spinal cord too and that spinal  
33      cord atrophy is indeed an important *in vivo* imaging biomarker contributing to understanding  
34      neurodegeneration associated with dementia.

35      **Methods:** 3DT1 images of 31 Alzheimer's disease (AD) and 35 healthy control (HC) subjects were  
36      processed to calculate volumes of brain structures and cross-sectional area (CSA) and volume  
37      (CSV) of the cervical cord (per vertebra as well as the C2-C3 pair (CSA23 and CSV23)). Correlated  
38      features ( $\rho > 0.7$ ) were removed, and best subset identified for patients' classification with the  
39      Random Forest algorithm. General linear model regression was used to find significant differences  
40      between groups ( $p <= 0.05$ ). Linear regression was implemented to assess the explained variance of  
41       $R^2$  and the  $p$  value of the explained variance.

## Spinal cord atrophy contribution to AD

46 the Mini Mental State Examination (MMSE) score as dependent variable with best features as  
47 predictors.

48 **Results:** Spinal cord features were significantly reduced in AD, independently of brain volumes.  
49 Patients classification reached 76% accuracy when including CSA23 together with volumes of  
50 hippocampi, left amygdala, white and grey matter, with 74% sensitivity and 78% specificity.  
51 CSA23 alone explained 13% of MMSE variance.

52 **Discussion:** Our findings reveal that C2-C3 spinal cord atrophy contributes to discriminate AD  
53 from HC, together with more established features. Results show that CSA23, calculated from the  
54 same 3DT1 scan as all other brain volumes (including right and left hippocampi), has a  
55 considerable weight in classification tasks warranting further investigations. Together with recent  
56 studies revealing that AD atrophy is spread beyond the temporal lobes, our result adds the spinal  
57 cord to a number of unsuspected regions involved in the disease. Interestingly, spinal cord atrophy  
58 explains also cognitive scores, which could significantly impact how we model sensorimotor  
59 control in degenerative diseases with a primary cognitive domain involvement. Prospective studies  
60 should be purposely designed to understand the mechanisms of atrophy and the role of the spinal  
61 cord in AD.

## Spinal cord atrophy contribution to AD

### 62 1 Introduction

63 Dementia is one of the most debilitating cognitive neurodegenerative disorders affecting the central  
64 nervous system in elderly people and having a significant impact on daily life activities. With an  
65 ageing population the incidence of dementia is growing and the consequences on society are huge.  
66 Clinically, several forms of dementia-like diseases that differently impair multiple cognitive and  
67 behavioral domains are defined. Alzheimer's disease (AD) is the most common cause of dementia  
68 and it is responsible for 60% to 80 % of cases worldwide<sup>1</sup>. What is the effect of neurodegeneration  
69 on sensorimotor control is an interesting question because it is believed to be highly relevant also  
70 for understanding cognitive functions. As the spinal cord is relaying sensorimotor control signals  
71 from the cortex to the peripheral nervous system and viceversa, it is indeed important to assess  
72 whether it is affected by atrophy in a disease that is known for its involvement of cognitive  
73 domains. Recent indications suggest that there is definitely a sensorimotor network rewiring and  
74 that the motor system may even be affected before cognitive functions in AD<sup>2-6</sup>. Clinical symptoms  
75 of early AD include amongst others fine motor impairment, with for example worsening of writing  
76 abilities. Therefore, it is important to understand first of all whether the spinal cord plays a part in  
77 this disease and to understand how significant is its involvement.

78 AD is associated with an extracellular deposit of  $\beta$ -amyloid plaques in the brain and cerebral  
79 vessels, but also to the presence of intracellular neurofibrillary tangles, which appear like paired  
80 helical filaments with hyperphosphorylated tau proteins. Tau tangles have been identified as the  
81 cause of cortical neurons' degeneration while  $\beta$ -amyloid oligomers have an important role in  
82 synaptic impairment, hence  $\beta$ -amyloid plaques deposition is suggested to raise later during the AD  
83 progression<sup>7,8</sup>. This neuronal degeneration explained by pathophysiology leads to macroscopic  
84 atrophy of specific brain structures, such as the hippocampi and the medial temporal lobes<sup>9</sup>, which  
85 can be detected using Magnetic Resonance Imaging (MRI) techniques. Indeed, several MRI studies  
86 have demonstrated significant atrophy of white matter, gray matter and specific brain structures  
87 such as the hippocampi, thalamus and amygdalae in AD patients suggesting that these structures are  
88 informative in identifying dementia disorders<sup>10,11</sup>. The hippocampi have been proposed as in vivo  
89 non-invasive imaging biomarkers of AD while other structures may be useful in distinguishing  
90 between different subtypes of dementia<sup>12</sup>. Only far and few old studies have looked at the spinal  
91 cord in AD, from a postmortem histochemical analysis and with reference to the autonomic system,  
92 but results were never reproduced or follow through as they focused on tau pathology, which was  
93 only sporadically reported<sup>13</sup>.

94 Recently, numerous MRI investigations have tried to identify new in vivo biomarkers for dementia  
95 to understand mechanisms of AD, to have better tools for assessing new therapies and predicting  
96 the clinical evolution of prodromic stages of dementia. Optical Coherence Tomography studies, for  
97 example, have been used to demonstrate that retinal ganglion cell degeneration can be associated to  
98 early stages of AD. Also, structures like the cerebellum, not classically associated with AD, have  
99 been found to be altered in imaging studies of dementia<sup>2</sup>, with atrophy of the anterior cerebellum -  
100 known for its motor control - being present even in the prodromic stages of mild cognitive  
101 impairment (MCI)<sup>14</sup>. A recent work has also looked at graph theory metrics to distinguish patterns  
102 of AD, identifying potentially different subtypes<sup>15</sup>, although focusing on cortical and deep grey  
103 matter areas, without including the cerebellum and the spinal cord. Studies of other diseases  
104 associated with neurodegeneration, such as multiple sclerosis<sup>16</sup>, amyotrophic lateral sclerosis<sup>17</sup>, and  
105 spinal cord injury<sup>18</sup>, have revealed that atrophy of the spinal cord is indicative of widespread  
106 alterations of the central nervous system and might be considered as a relevant imaging biomarker  
107 in a wider range of neurodegenerative diseases. Nevertheless, this kind of alteration has never been  
108 investigated and reported in dementia patients. Hence, the main aim of the present work was in the  
109 first instance to assess whether spinal cord volume is reduced in AD patients compared to healthy  
110 controls (HC), hypothesizing that the neurodegeneration typical of AD spreads to all components of  
111 the central nervous system; we achieved this by comparing a number of spinal cord features

## Spinal cord atrophy contribution to AD

113 between AD and HC. This information is very important for our understanding of how a  
114 neurodegenerative disease like AD has implications beyond the known brain atrophy: this could  
115 also have significant impact on future modeling of brain networks. Furthermore, in case of a  
116 positive outcome, it is important to quantify the role of spinal cord features in distinguishing  
117 between AD and HC to drive the design of future studies; for this we implemented a machine  
118 learning approach for features selection, that is increasingly applied to improve diagnostic accuracy  
119 by quantitative imaging<sup>19,20</sup>. Finally, we quantified the contribution of spinal cord atrophy to  
120 explain variance of clinical scores for determining its clinical relevance.

## 121 2 Materials and Methods

### 123 2.1 Subjects

124 A total of 66 subjects including 31 AD patients (age  $(73 \pm 7)$  years, 12 females (F), MMSE =  $16 \pm$   
125 6) and 35 HC (age  $(69 \pm 10)$  years, 17 F, MMSE =  $28 \pm 1$ ), as a reference group, were analyzed. 7  
126 subjects (4 HC and 3 AD) were excluded from the study due to post-processing issues, hence the  
127 final dataset comprised 32 HC and 28 AD.

128 Inclusion criteria for patients were: clinical diagnosis of dementia on the basis of the Diagnostic and  
129 Statistical Manual of Mental Disorders (DSM-5) criteria<sup>21</sup>, Mini-Mental State Examination  
130 (MMSE) score<sup>22</sup> below 24 and age above 60 years. Exclusion criteria comprised the presence of at  
131 least one of the following: epilepsy or isolated seizures, major psychiatric disorders over the  
132 previous 12 months, pharmacologically treated delirium or hallucinations, ongoing alcoholic abuse,  
133 acute ischemic or hemorrhagic stroke, known intracranial lesions, and systemic causes of subacute  
134 cognitive impairment<sup>23</sup>. Diagnosis of AD was made according to the criteria of the National  
135 Institute of Neurological and Communicative Disorders and Stroke and Alzheimer's Disease and  
136 Related Disorders Association (NINCDS-ADRDA) workgroup<sup>24</sup>. HC were enrolled on a voluntary  
137 basis among subjects with MMSE score above 27 and attending a local third age university  
138 (University of Pavia, Information Technology course) or included in a program on healthy ageing  
139 (Fondazione Golgi, Abbiategrasso, Italy).

140 The study was accomplished in accordance with the Declaration of Helsinki and with the  
141 approbation of the local ethic committee of the IRCCS Mondino Foundation, upon signature of the  
142 written informed consent by the subjects.

### 143 2.2 MRI Acquisition

144 High resolution 3D T1-weighted(3DT1-w) MR images were acquired using a Siemens  
145 MAGNETOM Skyra3T(Siemens AG, Erlangen, Germany) with software version  
146 NUMARIS/4(syngo MR D13C version) and a receiving head-coil with 32 channels.

147 Scan parameters were<sup>12</sup>: TR=2300ms, TE=2.95ms, TI=900 ms, flip angle=9degrees, field of view  
148 (FOV)=269x252mm, acquisition matrix=256x240, in-plane resolution=1.05x1.05mm, slice  
149 thickness=1.2 mm, and 176 sagittal slices. The FOV, in feet-to-head direction, was set to cover the  
150 entire brain and cervical cord up to the C5 vertebra in all subjects.

### 151 2.3 Spinal Cord analysis

152 For each subject, the 3DT1-w volume (the same used normally for brain atrophy measurements -  
153 see below) was resized removing the brain and centering the FOV on the spine. Once a single  
154 volume of interest (VOI) comprising the same spinal cord regions for each 3DT1-w was defined  
155 (matrix=176x240x96 voxels), the process was automatized for the whole dataset. The resized  
156 3DT1-w volumes were analyzed with the Spinal Cord Toolbox ([http://sourceforge.net](http://sourceforge.net/projects/spinalcordtoolbox)  
157 /projects/spinalcordtoolbox), an open source software specifically developed to elaborate spinal  
158 cord images, to extract features of the C1-C5 vertebrae.

159 The spinal cord was segmented with the *propseg* algorithm<sup>25</sup> and manually labelled<sup>26</sup> to identify all  
160 vertebrae separately<sup>27</sup>(Figure 1). Mean cross-sectional area (CSA) and volume (CSV) were

## Spinal cord atrophy contribution to AD

163 calculated for each vertebra and for the C2-C3 pair<sup>28,29</sup>(CSA23 and CSV23), given the known  
164 sensitivity of this combined level to disease severity<sup>30</sup>. CSA is computed by counting pixels in each  
165 slice and then geometrically adjusting it multiplying by the angle (in degrees) between the spinal  
166 cord centerline and the inferior-superior direction. CSV, indeed, is computed by counting pixels and  
167 multiplying by slice thickness.  
168

### 169 2.4 Brain atrophy analysis

170 The 3DT1-w images were also segmented into white matter (WM), gray matter (GM) and  
171 cerebrospinal fluid (CSF) using SPM12 (<https://www.fil.ion.ucl.ac.uk/spm/software/spm12>)<sup>31</sup>,  
172 while left (L) and right (R) hippocampi (LHip and RHip), thalamus (LThal and RThal) and  
173 amygdalae (LAmy and RAmy) were segmented using FIRST (FSL,  
174 <https://fsl.fmrib.ox.ac.uk/fsl/fslwiki/FIRST>)<sup>32</sup> (Figure 2).

175 WM, GM and all other brain structures volumes were calculated in mm<sup>3</sup>. Total intracranial volume,  
176 as the sum of WM, GM and CSF, was also calculated to account for different brain sizes.  
177

### 178 2.5 Classification of AD and feature selection analysis

179 Classification between AD and HC was performed using a machine learning approach implemented  
180 in Orange (<https://orange.biolab.si/>).

181 A total of 22 features were extracted from the above MRI morphometric analysis. Given the large  
182 number of parameters extracted compared to the sample size of our AD and HC groups, a feature  
183 reduction approach was adopted in order to control for overfitting issues. The Spearman correlation  
184 coefficient<sup>33</sup> was obtained in Matlab between pairs of all calculated metrics. When pairs of metrics  
185 had a correlation coefficient greater than 0.7, one metric was kept while the other was eliminated.

186 Ranking was implemented with the ReliefF algorithm<sup>34</sup> on the uncorrelated features to identify  
187 the best subset able to classify AD from HC, and particularly to investigate the contribution of  
188 spinal cord metrics to the task. In order to identify a unique subset of features, 30% of instances was  
189 employed for ranking. Data were normalized by span to avoid a polarization of the results due to the  
190 different scale of features, as for WM compared to CSA. The remaining 70% of instances was  
191 further divided into 70% for the Random Forest algorithm application and 30% to test its  
192 classification accuracy (CA=(True Positive + True Negative)/( True Positive + True Negative +  
193 False Positive + False Negative)), sensitivity (Sens= True Positive/(True Positive + False negative))  
194 and specificity (Spec= True Negative/(True Negative + False Positive)) , using the previously-  
195 identified best features.

196 Among several machine learning algorithms, RF was selected for its robustness against a reduced  
197 number of input features and the capacity to weight features runtime, providing features relevance  
198 in a classification task<sup>35,36</sup>. The Receiving Operating Characteristics (ROC) curve was then obtained  
199 to visually discriminate between AD and HC and the Area Under the Curve was also calculated to  
200 quantify the overall ability of RF to discriminate between AD and HC.  
201

### 202 2.6 Statistical analysis

203 Statistical tests were performed using the Statistical Package For Social Sciences (SPSS) software,  
204 version 21 (IBM, Armonk, New York). All continuous data were tested for normality using a  
205 Shapiro-Wilk test<sup>37</sup>. Age and MMSE were compared between AD and HC using a two-tailed  
206 Kruskal-Wallis test<sup>38</sup> while gender was compared using a chi-squared test<sup>39</sup>. A multivariate  
207 regression model with gender, age and total intracranial volume as covariates was used to compare  
208 all morphometric metrics between AD and HC. Two-sided  $p<0.05$  was considered statistically  
209 significant.

210 Furthermore, to assess the power of the best features in explaining the variance of the MMSE, a  
211 linear regression model was implemented using the MMSE score as the dependent variable and the

## Spinal cord atrophy contribution to AD

212 best features as predictors. These independent features were used in two ways: i) each predictor was  
213 used alone to determine its specific contribution to MMSE; ii) all features were used in a backward  
214 approach to identify which of them explained the greatest percentage of MMSE variance. A  
215 threshold of  $p < 0.01$  (two-tailed) was considered statistically significant.

### 216 3 Results

#### 218 3.1 Subjects

219 Population demographics and neuropsychological scores are reported in Table 1. Significant  
220 differences were found in MMSE between HC and AD patients.

221

#### 222 3.2 Morphometric changes in AD patients

223 All results are reported in Table 2 and Table 3. AD patients compared to HC showed atrophy in all  
224 brain structures. Moreover, all patients for all investigated spinal cord segments showed reduced  
225 CSA at all vertebral levels, while CSV was significantly reduced only in correspondence of  
226 vertebrae C1 and C2.

227

#### 228 3.3 AD classification based on morphometric data

229 Results of the correlation analysis are reported in Figure 3, and show that brain volumes are not  
230 significantly correlated with spinal cord metrics.

231 Features that were considered independent from each other and that were entered in the feature  
232 selection analysis are reported in Table 4. The best features selected by the RF algorithm for the AD  
233 versus HC classification task are reported in Table 5 and include: RHip, WM, LAmy, LHip,  
234 CSA23, GM. Interestingly, CSA23 was identified as one of the most informative features to  
235 distinguish AD patients from HC. RF outcomes are reported in Table 6 and showed that the  
236 classification accuracy of AD patients is 76%, sensitivity 74% and specificity 78%. The Area Under  
237 Curve (AUC) percentage reached 86%, showing a remarkable classification performance of the RF  
238 algorithm to distinguish AD from HC subjects. Moreover, it is noticeable that the hippocampi have  
239 dominant weight, but that there is a relevant contribution to the classification from CSA23.

240

#### 241 3.4 MMSE and morphometric data relationship

242 The combination of the six best features, including WM, RHip, LHip, LAmy, CSA23 and GM,  
243 explained 44% of the overall variance of the MMSE. The function equation describing the linear  
244 model obtained by the regression analysis included the following terms with their weights:  
245  $0.329 \times LHip - 0.145 \times RHip + 0.145 \times LAmy + 0.064 \times CSA23 - 0.227 \times GM + 0.557 \times WM$ . The  
246 MMSE explained variance was progressively reduced by simplifying the model, i.e. removing one or more  
247 predictors, as shown in Table 7. Each separate feature significantly ( $p < 0.005$ ) explained a  
248 percentage of MMSE variance ranging between 13% to 36%. The feature that most explains MMSE  
249 variance was the WM volume (36%), with CSA explaining 13%.

### 250 4 Discussions

251 The present work is pioneering the investigation of spinal cord alterations in patients with dementia,  
252 and in particular with AD, a major neurodegenerative disease known for its profound effect on  
253 cognitive functions. The motor/sensorimotor system has already been shown to be affected in AD at  
254 various levels in the brain, but nobody has yet investigated the spinal cord to date<sup>2-6</sup>. Here we have  
255 shown that the spinal cord is very atrophic indeed, at least in established AD patients. This is an  
256 important finding, as it demonstrates that atrophy and neurodegeneration is widespread beyond  
257 areas with excellent standards such as the hippocampi and temporal lobes. Our results are, indeed,  
258 consistent with the fact that patients present significantly different brain volumes with respect to  
259 HC, and all segmented brain structures, except for the right amygdala, are statistically significantly  
260 atrophic in AD. In this context, our work goes further and demonstrates that volumes of all cervical

## Spinal cord atrophy contribution to AD

vertebral segments are reduced in AD, with the CSV of the first and second vertebrae being significantly atrophic with respect to HC. These results are coherent with results obtained for cerebral structures and suggest the existence of a remarkable reduction (of the order of 10%) in the volume of the spinal cord in dementia. This hypothesis is further supported by significant CSA reduction for all vertebrae in patients, with CSA being calculated considering the curvature of the spinal cord<sup>28</sup>. Previous studies have reported spinal cord atrophy in patients with neurological diseases<sup>40,41</sup>, such as multiple sclerosis with focal lesions in the brain and spinal cord, but to date no studies have explored the existence of a volumetric loss of spinal cord tissue in dementia. This finding has implications for how we think about the relationship between the cognitive and sensorimotor systems, which we have shown to be conjointly affected in established AD. Not to forget that the spinal cord is also the relay of the autonomic system that has been reported as dysfunctional in AD<sup>42-44</sup>.

Post mortem studies of AD patients will be needed to confirm the biophysical source of spinal cord atrophy, although at first one could imagine that any change in CSA and CSV could be the result of retrograde Wallerian degeneration from the cerebral cortex<sup>45</sup>. Given that we have also demonstrated that spinal cord features are independent of brain volumes, it cannot be excluded that alterations in spinal cord morphometric measurements (CSA and CSV) in AD are the result of primary retrogenesis linked to myelin and axonal pathology. It is indeed very significant that a recent study of the 5xFAD animal model of AD shows amyloid plaques accumulation in the spinal cord tissue, with a particular concentration at cervical level and a time dependent accumulation that starts 11 weeks from onset; interestingly, the same study found independent and extensive myelinopathy, while the motoneurons count at 6 months was not altered compared to the wild type<sup>46</sup>. While we cannot be conclusive on the mechanisms of spinal cord atrophy in AD, our results are intriguing and calling for larger studies of prodromic subjects to be followed over time; such studies would also confirm whether the suggestion that the motor system (neocortex, cerebellum and spinal cord) is affected even before the cognitive one can be substantiated<sup>3,5,14</sup>

A further result of our work is that of all spinal cord features analysed here, the area of vertebra C2-C3 (CSA23) significantly contributes to discriminate between HC and AD patients. Usually, only atrophy of brain regions is investigated in dementia<sup>47,48</sup>. Indeed, spinal cord morphometric measures (CSA and CSV) alone cannot directly discriminate between AD and HC, but CSA23 was identified as one of the six best features useful to distinguish between these groups of subjects. Classifier accuracy was good and reached its best performance, around 76%, when both volume of brain structures, such as LHip and RHip (considered biomarkers of AD progression<sup>49</sup>), WM and GM, as well as spinal cord CSA23 were included in the classification procedure. In addition, the ROC curve between AD and HC (shown in Figure 4) reported high performance with AUC of 86%. The sensitivity and specificity of the RF algorithm, reaching 74% and 78% respectively, showed a remarkable ability in correctly identify healthy and pathological cases. Examining the RF feature weighting (reported in Table 6) it is also noticeable that CSA23 had weight higher than GM, highlighting that it should be considered as an additional biomarker together with the more conventional volumes of subcortical regions<sup>39</sup>. These results indicate the yet unexplored potential influence that spinal cord features can play in the classification of dementia in line with recent publications, which have recognized that other brain structures play a key role in identifying AD patients and in distinguishing between different subtypes of dementia<sup>12,15</sup>.

Regarding the fact that CSA23 emerged as being particularly sensitive to pathological changes in AD is in accordance with other studies in neurodegenerative diseases such as amyotrophic lateral sclerosis<sup>17</sup> and could be seen as a corroborating evidence of a correlation between spinal cord atrophy and neurodegeneration. In light of the only animal model study reported to date<sup>46</sup>, which shows that C2-C3 is selectively affected by greater morphological biophysical alterations, our

## Spinal cord atrophy contribution to AD

309 results become of remarkable value. Moreover, upper limb sensorimotor impairment is known to be  
310 clinically relevant in early AD, which is substantiating the relevance of our finding and calls for  
311 future investigations involving correlations with sensorimotor scores and purposely designed  
312 prospective studies to answer mechanistic questions.

313 Finally, our data show that also clinical aspects of AD are partially explained by spinal cord  
314 atrophy. Given the exploratory nature of the present study, we assessed whether spinal cord atrophy  
315 could be correlated with the variance of the MMSE, which is a global test, clinically used to assess  
316 AD severity. We found that 43% of the MMSE variance was explained with a multiple regression  
317 model implemented with all the best features included as independent variables, whereas CSA23  
318 alone explained 13% of the MMSE variance, which is a considerable contribution indeed.

319 From a methodological point of view, we know that evaluating spinal cord alterations in humans in  
320 vivo is challenging due to technical and anatomical constraints, including subject positioning inside  
321 the scanner, individual subject's neck curvature or subject's motion. Furthermore, the spinal cord is  
322 a small structure and optimized sequences with reduced FOV and appropriate alignment should be  
323 used to obtain reproducible results<sup>50</sup>. Dedicated acquisition protocols would also allow one to  
324 analyse specific alterations of spinal cord GM and WM, that were not available with the present  
325 data that used 3DT1-w scans, used for whole-brain or regional brain volume calculations, to extract  
326 spinal cord features<sup>51,52</sup>. Regarding feature selection and classification, we know that recent studies  
327 have combined several MRI findings with machine learning approaches to attempt the classification  
328 of dementia subtypes and prediction of disease progression. Accuracy of about 80%<sup>53,54</sup> was  
329 achieved when AD and HC were classified while more fluctuating results were reported when more  
330 subtypes of dementia were considered. In the present study a RF algorithm with the "leave-one-out"  
331 approach was chosen to discriminate between AD and HC because RF is robust with small numbers  
332 of subjects and performs features weighting runtime with good sensitivity and specificity.

333 Given the nature of this prospective study, it was not possible to investigate the involvement of the  
334 spinal cord at different stages of AD or in different types of dementia to explore its full clinical  
335 potentials. Therefore, a comprehensive battery of sensorimotor and cognitive tests should be  
336 performed to understand how the clinical and MRI pictures are evolving during the disease  
337 progression and to establish when spinal cord atrophy occurs and its clinical weight. It is also  
338 essential to promote multi-modal studies that can disentangle the contribution of myelin, amyloid  
339 accumulation, axonal swelling and axonal loss to brain and spinal cord alterations in  
340 neurodegenerative diseases to understand local and global mechanisms of damage.

341 In conclusion, the present work can be considered a milestone because for the first time it  
342 demonstrates in a cohort of AD and HC subjects the contribution of spinal cord atrophy to explain  
343 clinical indicators of dementia and to improve disease classification, opening also mechanistic  
344 questions for future studies. It is indeed important that we rethink in particular of how the  
345 sensorimotor and cognitive systems are affected by AD, integrating spinal cord with brain  
346 information, including the temporal lobes with the hippocampi, the motor and sensorimotor  
347 cortices, the limbic system with the amygdala and the cerebellum, which we now know are all  
348 implicated in AD.

## Spinal cord atrophy contribution to AD

### 350 5 Tables

351  
352 **Table 1: Subjects' demographic and neuropsychological data**

	HC (n=32)	AD (n=28)	p-value
	mean (SD)	mean (SD)	
Age [yrs]	69.4 (9.6)	73.0 (6.4)	0.138
Gender (Male [%])	51.4	56.2	0.800
MMSE	28.5 (0.2)	16.0 (1.1)	< 0.001*

353  
354 Gender is expressed in Male % and compared with a Chi-square test. Age and MMSE are expressed as mean (SD) and  
355 compared with a Kruskall-Wallis test. Significance was set to p=0.05. \* refers to statistically significant comparisons.  
356

## Spinal cord atrophy contribution to AD

357

358 **Table 2: Brain morphometric changes in AD patients**

Brain Structures (mm <sup>3</sup> )	HC (n=32)	AD (n=28)	p-value
	mean (SD)	mean (SD)	
ICV	1573086 (144439)	1511611 (139532)	0.04*
WM	612335 (11230)	540237 (12064)	<0.001*
GM	427508 (6492)	399274 (6975)	0.006*
RHip	3602 (106)	2932 (114)	<0.001*
LHip	3591 (99)	2822 (107)	<0.001*
LThal	7013 (109)	6433 (118)	0.001*
RThal	6808 (109)	6371 (117)	0.011*
LAmy	1256 (41)	1054 (44)	0.002*
RAmy	1323 (63)	1120 (66)	0.035*

359

360 Volumes of different brain structures expressed in mm<sup>3</sup>. Values are expressed as mean (SD). Significance was set at p =  
361 0.050. \* refers to statistically significant values.

362

## Spinal cord atrophy contribution to AD

363 **Table 3: Spinal cord morphometric changes in AD patients**

Vertebra	HC (n=32)	AD (n=28)	p-value
	mean (SD)	mean (SD)	
Area (mm <sup>2</sup> )	C1	69.8 (1.6)	63.1 (1.8)
	C2	65.7 (1.3)	60.2 (1.4)
	C3	62.5(1.4)	56.9 (1.6)
	C4	62.5 (1.6)	57.2 (1.7)
	C5	58.9 (1.6)	52.8 (1.7)
	C2-C3	65.1 (1.6)	58.3 (1.7)
Volume (mm <sup>3</sup> )	C1	883.4 (27.3)	800.4 (29.3)
	C2	979.8 (28.4)	857.1 (30.6)
	C3	932.3 (29)	886.9 (31.2)
	C4	882.3 (35.1)	807.9 (37.7)
	C5	667 (34.5)	609.1 (37.1)
	C2-C3	1860.5 (66.8)	1729.9 (71.7)

364  
365  
366  
367

Cross sectional area (in mm<sup>2</sup>) and volumes (in mm<sup>3</sup>) of spinal cord vertebrae. Values are expressed as mean (SD).

Significance was set at p = 0.050. \* refers to statistically significant values.

## Spinal cord atrophy contribution to AD

368

**Table 4: Cerebral and spinal cord morphometric metrics**

Set of all calculated Metrics				Set of uncorrelated metrics		
Brain	Spine	Personal		Brain	Spine	Personal
WM	CSA1	CSV1	Age	WM	-	-
GM	CSA2	CSV2	Gender	GM	-	-
RHip	CSA3	CSV3		LHip	-	CSV3
LHip	CSA4	CSV4		RHip	-	-
RThal	CSA5	CSV5		-	-	CSV5
LThal	CSA23	CSV23		-	CSA23	-
RAmy				-		
LAmy				LAmy		

369

370 Left column: initial dataset of morphometric metrics. Right column: subset of uncorrelated morphometric metrics.  
371 WM=white matter, GM=gray matter, RHip=right hippocampus, LHip=left hippocampus, RThal=right thalamus,  
372 LThal=left thalamus, RAmy=right amygdala, LAmy=left amygdala, CSA=cross sectional area, CSV=cross sectional  
373 volume  
374

## Spinal cord atrophy contribution to AD

375 **Table 5: Features ranking**

Features	Weight
RHip	0.1125
WM	0.0630
LAmy	0.0629
LHip	0.0615
CSA23	0.0317
GM	-0.0041

376

377 9 HC and 9 AD patients were used in the ranking procedure. Ranking Algorithm: ReliefF applied on a dedicated subset  
378 (30% of instances, number of neighbors = 10).

379

## Spinal cord atrophy contribution to AD

380  
381  
382

**Table 6: Random Forest classification**

<b>Performance</b>	
<b>Accuracy</b>	76 %
<b>Sensitivity</b>	74%
<b>Specificity</b>	78%
<b>Area Under Curve</b>	86%
<b>Feature</b>	<b>RF weight</b>
<b>LHip</b>	9.039
<b>RHip</b>	2.734
<b>LAmy</b>	2.263
<b>CSA23</b>	1.828
<b>WM</b>	0.323
<b>GM</b>	0.060

383  
384 23 HC and 19 AD were used to test classifier performance. A leave-one-out procedure was used to test the performance  
385 of Random Forest (RF) with the best feature subset reported in table 5. RF features weight are also reported.  
386

## Spinal cord atrophy contribution to AD

387  
388  
389

**Table 7: MMSE outcomes**

	Explained Variance	Influence Significance
<b>Multiple Linear Model</b>		
MMSE = $\beta_1 \cdot \text{LHip} + \beta_2 \cdot \text{RHip} + \beta_3 \cdot \text{LAmy} + \beta_4 \cdot \text{CSA23} + \beta_5 \cdot \text{GM} + \beta_6 \cdot \text{WM}$	44%	<0.001
MMSE = $\beta_1 \cdot \text{LHip} + \beta_2 \cdot \text{RHip} + \beta_3 \cdot \text{LAmy} + \beta_4 \cdot \text{GM} + \beta_5 \cdot \text{WM}$	43%	<0.001
MMSE = $\beta_1 \cdot \text{LHip} + \beta_2 \cdot \text{LAmy} + \beta_3 \cdot \text{GM} + \beta_4 \cdot \text{WM}$	43%	<0.001
MMSE = $\beta_1 \cdot \text{LHip} + \beta_2 \cdot \text{GM} + \beta_3 \cdot \text{WM}$	42%	<0.001
MMSE = $\beta_1 \cdot \text{LHip} + \beta_2 \cdot \text{WM}$	40%	<0.001
<b>Linear Model</b>		
MMSE = $\beta \cdot \text{WM}$	36%	<0.001
MMSE = $\beta \cdot \text{LHip}$	30%	<0.001
MMSE = $\beta \cdot \text{RHip}$	22%	<0.001
MMSE = $\beta \cdot \text{GM}$	17%	0.001
MMSE = $\beta \cdot \text{LAmy}$	16%	0.001
MMSE = $\beta \cdot \text{CSA23}$	13%	0.005

390  
391  
392  
393

MMSE Linear Regression Models. The model-explained variance is calculated with the R<sup>2</sup> index. Significance was set to p=0.05; all described model showed statistically significant influence (ANOVA).

## Spinal cord atrophy contribution to AD

### 394 6 Figures Legend

395

396 **Figure 1.** Labelled vertebrae in two randomly chosen subjects: a HC subject on the left and an AD  
397 patient on the right (slice n=96, sagittal plane). Each color represents a different vertebra from C1  
398 (yellow) to C5 (fuchsia).

399 **Figure 2.** Cerebral tissue segmentation in two randomly chosen subjects: a HC subject on the left  
400 and an AD patient on the right. Top row: WM (yellow) and GM (blue) segmentation (slice n = 126,  
401 transverse plane). Middle row: hippocampi (yellow) and amygdalae (light blue) segmentation (slice  
402 n = 123, transverse plane). Bottom row: thalami (green) segmentation (slice n = 132, transverse  
403 plane).

404 **Figure 3.** Correlation matrix between pairs of variables, tested with the Spearman's correlation  
405 coefficient. All correlations for  $p < 0.5$  are set to white, correlations for  $p > 0.5$  are red to yellow, with  
406 yellow ( $p=1$ ) being the strongest correlation. No spinal cord metrics are correlating with brain  
407 metrics with  $p > 0.7$ , which is the threshold we used for extracting the set of uncorrelated features  
408 (Table 1)

409 **Figure 4.** ROC curves for AD-HC classification using Random Forest feature selection.  
410 Pathological class (AD = 1) was considered as the target class. The curve shows higher  
411 performance (bold red line) than the majority algorithm (diagonal). TN rate is the rate of true  
412 negative and FP rate is the rate of false positives.

413

## Spinal cord atrophy contribution to AD

### 414 7 Acknowledgements

415

416 We thank University of Pavia and Mondino Foundation (Pavia, Italy) for funding; The UK Multiple  
417 Sclerosis Society and UCL-UCLH Biomedical Research Centre for ongoing support of the Queen  
418 Square MS Centre. CGWK receives funding from ISRT, Wings for Life and the Craig H. Neilsen  
419 Foundation(the INSPIRED study), from the MS Society(#77), Wings for Life(#169111),  
420 Horizon2020(CDS-QUAMRI, #634541). This research has received funding from the European  
421 Union's Horizon 2020 Framework Programme for Research and Innovation under the Specific  
422 Grant Agreement No.785907(Human Brain Project SGA2) for the work of FP and ED. ECTRIMS  
423 and the Multiple Sclerosis International Federation(MSIF) supported the work of GC with funding  
424 (ECTRIMS Postdoctoral Research Fellowship Program, MSIF Du Pré grant).

### 425 8 Authorship

426 CGWK, ED, FP and RL conceptualized the study. FP and RL designed and performed the analyses  
427 with support from GC. PV and NA acquired all MRI data. ES and SB acquired all  
428 neuropsychological data helping for data interpretation. AC, ES and GM enrolled all patients and  
429 performed all clinical evaluations. CGWK and ED provided support and guidance with data  
430 interpretation with clinical contribution of all physicians. CGWK, FP and RL wrote the manuscript,  
431 with comments from all other authors.

### 432 9 Conflict of interest

433 The authors declare that the research was conducted in the absence of any commercial or financial  
434 relationship that could be construed as a potential conflict of interest.

435

## Spinal cord atrophy contribution to AD

436 10 **References**

437 1. Kumar A, Singh A, Ekavali. A review on Alzheimer's disease pathophysiology and its  
438 management: An update [Internet]. *Pharmacol. Reports* 2015;67(2):195–203. Available from:  
439 <http://dx.doi.org/10.1016/j.pharep.2014.09.004>

440 2. Castellazzi G, Palesi F, Casali S, et al. A comprehensive assessment of resting state  
441 networks: Bidirectional modification of functional integrity in cerebro-cerebellar networks in  
442 dementia. *Front. Neurosci.* 2014;8(8 JUL):1–18.

443 3. Albers MW, Gilmore GC, Kaye J, et al. At the interface of sensory and motor dysfunctions  
444 and Alzheimer's disease. *Alzheimer's Dement.* 2015;11(1):70–98.

445 4. Fu L, Liu L, Zhang J, et al. Brain Network Alterations in Alzheimer's Disease Identified by  
446 Early-Phase PIB-PET. *Contrast Media Mol. Imaging* 2018;2018:6830105.

447 5. Agosta F, Rocca MA, Pagani E, et al. Sensorimotor network rewiring in mild cognitive  
448 impairment and Alzheimer's disease. *Hum. Brain Mapp.* 2010;31(4):515–525.

449 6. Salustri C, Tecchio F, Zappasodi F, et al. Sensorimotor Cortex Reorganization in  
450 Alzheimer's Disease and Metal Dysfunction: A MEG Study. *Int. J. Alzheimers. Dis.*  
451 2013;2013:638312.

452 7. Song H-L, Shim S, Kim D-H, et al. beta-Amyloid is transmitted via neuronal connections  
453 along axonal membranes. *Ann. Neurol.* 2014;75(1):88–97.

454 8. Šimić G, Babić Leko M, Wray S, et al. Tau protein hyperphosphorylation and aggregation in  
455 alzheimer's disease and other tauopathies, and possible neuroprotective strategies.  
456 *Biomolecules* 2016;6(1):2–28.

457 9. Scher AI, Xu Y, Korf ESC, et al. Hippocampal morphometry in population-based incident  
458 Alzheimer's disease and vascular dementia: The HAAS. *J. Neurol. Neurosurg. Psychiatry*  
459 2011;82(4):373–376.

460 10. Stonnington CM, Chu C, Klöppel S, et al. Predicting clinical scores from magnetic resonance  
461 scans in Alzheimer's disease [Internet]. *Neuroimage* 2010;51(4):1405–1413. Available from:  
462 <http://dx.doi.org/10.1016/j.neuroimage.2010.03.051>

463 11. Pini L, Pievani M, Bocchetta M, et al. Brain atrophy in Alzheimer's Disease and aging  
464 [Internet]. *Ageing Res. Rev.* 2016;30:25–48. Available from:  
465 <http://dx.doi.org/10.1016/j.arr.2016.01.002>

466 12. Palesi F, De Rinaldis A, Vitali P, et al. Specific patterns of white matter alterations help  
467 distinguishing Alzheimer's and vascular dementia. *Front. Neurosci.* 2018;12(APR)

468 13. Engelhardt E, Laks J. Alzheimer disease neuropathology:understanding autonomic  
469 dysfunction. *Dement. Neuropsychol.* 2016;2(3):183–191.

470 14. Toniolo S, Serra L, Olivito G, et al. Patterns of Cerebellar Gray Matter Atrophy Across  
471 Alzheimer's Disease Progression. *Front. Cell. Neurosci.* 2018;12:430.

472 15. Ferreira D, Pereira JB, Volpe G, Westman E. Subtypes of Alzheimer's Disease Display  
473 Distinct Network Abnormalities Extending Beyond Their Pattern of Brain Atrophy. *Front.*  
474 *Neurol.* 2019;10:524.

475 16. Liu Z, Yaldizli Ö, Pardini M, et al. Cervical cord area measurement using volumetric brain  
476 magnetic resonance imaging in multiple sclerosis [Internet]. *Mult Scler Relat Disord*  
477 2015;4(1):52–57. Available from: <http://dx.doi.org/10.1016/j.msard.2014.11.004>

478 17. Antonescu F, Adam M, Popa C, Tuță S. A review of cervical spine MRI in ALS patients.  
479 [Internet]. *J. Med. Life* 2018;11(2):123–127. Available from:  
480 <http://www.ncbi.nlm.nih.gov/pubmed/30140318%0Ahttp://www.ncbi.nlm.nih.gov/arti>

## Spinal cord atrophy contribution to AD

## Spinal cord atrophy contribution to AD

526 34. Urbanowicz RJ, Meeker M, La Cava W, et al. Relief-based feature selection: Introduction  
527 and review. *J. Biomed. Inform.* 2018;85:189–203.

528 35. Goel E, Abhilasha E. Random Forest: A Review. *Int. J. Adv. Res. Comput. Sci. Softw. Eng.*  
529 2017;7(1):251–257.

530 36. Breiman L. Random Forests [Internet]. *Mach. Learn.* 2001;45(1):5–32. Available from:  
531 <https://doi.org/10.1023/A:1010933404324>

532 37. Shapiro SS, Wilk MB. An Analysis of Variance Test for Normality (Complete Samples)  
533 [Internet]. *Biometrika* 1965;52(3/4):591–611. Available from:  
534 <http://www.jstor.org/stable/2333709>

535 38. Kruskal WH, Wallis WA. Use of Ranks in One-Criterion Variance Analysis [Internet]. *J.*  
536 *Am. Stat. Assoc.* 1952;47(260):583–621. Available from:  
537 <http://www.jstor.org/stable/2280779>

538 39. Pearson K. X. On the criterion that a given system of deviations from the probable in the case  
539 of a correlated system of variables is such that it can be reasonably supposed to have arisen  
540 from random sampling [Internet]. London, Edinburgh, Dublin Philos. Mag. J. Sci.  
541 1900;50(302):157–175. Available from: <https://doi.org/10.1080/14786440009463897>

542 40. Okuda DT, Melmed K, Matsuwaki T, et al. Central neuropathic pain in MS is due to distinct  
543 thoracic spinal cord lesions. *Ann. Clin. Transl. Neurol.* 2014;1(8):554–561.

544 41. Azodi S, Nair G, Enose-Akahata Y, et al. Imaging spinal cord atrophy in progressive  
545 myelopathies: HTLV-I-associated neurological disease (HAM/TSP) and multiple sclerosis  
546 (MS). *Ann. Neurol.* 2017;82(5):719–728.

547 42. Allan LM. Diagnosis and Management of Autonomic Dysfunction in Dementia Syndromes  
548 [Internet]. *Curr. Treat. Options Neurol.* 2019;21(8):38. Available from:  
549 <http://link.springer.com/10.1007/s11940-019-0581-2>

550 43. Allan LM, Ballard CG, Allen J, et al. Autonomic dysfunction in dementia. 2007;671–677.

551 44. Algotsson A, Viitanen M, Winblad B, Solders G. Autonomic dysfunction in Alzheimer's  
552 disease. *Acta Neurol. Scand.* 1995;91(1):14–18.

553 45. Alves GS, Oertel Knochel V, Knochel C, et al. Integrating retrogenesis theory to Alzheimer's  
554 disease pathology: insight from DTI-TBSS investigation of the white matter microstructural  
555 integrity. *Biomed Res. Int.* 2015;2015:291658.

556 46. Chu T-H, Cummins K, Sparling JS, et al. Axonal and myelinic pathology in 5xFAD  
557 Alzheimer's mouse spinal cord. *PLoS One* 2017;12(11):e0188218.

558 47. Štepán-Buksowska I, Szabó N, Horínek D, et al. Cortical and Subcortical Atrophy in  
559 Alzheimer Disease: Parallel Atrophy of Thalamus and Hippocampus [Internet]. *Alzheimer*  
560 *Dis. Assoc. Disord.* 2014;28(1) Available from:  
561 [https://journals.lww.com/alzheimerjournal/Fulltext/2014/01000/Cortical\\_and\\_Subcortical\\_At](https://journals.lww.com/alzheimerjournal/Fulltext/2014/01000/Cortical_and_Subcortical_At)  
562 [rophy\\_in\\_Alzheimer.10.aspx](https://journals.lww.com/alzheimerjournal/Fulltext/2014/01000/Cortical_and_Subcortical_Atrophy_in_Alzheimer.10.aspx)

563 48. Tardif CL, Devenyi GA, Amaral RSC, et al. Regionally specific changes in the hippocampal  
564 circuitry accompany progression of cerebrospinal fluid biomarkers in preclinical Alzheimer's  
565 disease. *Hum. Brain Mapp.* 2018;39(2):971–984.

566 49. O'Callaghan C, Shine JM, Hodges JR, et al. Hippocampal atrophy and intrinsic brain  
567 network dysfunction relate to alterations in mind wandering in neurodegeneration. *Proc.*  
568 *Natl. Acad. Sci. U. S. A.* 2019;

569 50. De Leener B, Lévy S, Dupont SM, et al. SCT: Spinal Cord Toolbox, an open-source software  
570 for processing spinal cord MRI data [Internet]. *Neuroimage* 2017;145(October 2016):24–

## Spinal cord atrophy contribution to AD

571 43. Available from: <http://dx.doi.org/10.1016/j.neuroimage.2016.10.009>

572 51. Fonov VS, Le Troter A, Taso M, et al. Framework for integrated MRI average of the spinal  
573 cord white and gray matter: the MNI-Poly-AMU template. *Neuroimage* 2014;102 Pt 2:817–  
574 827.

575 52. Levy S, Benhamou M, Naaman C, et al. White matter atlas of the human spinal cord with  
576 estimation of partial volume effect. *Neuroimage* 2015;119:262–271.

577 53. Waser M, Benke T, Dal-Bianco P, et al. Neuroimaging markers of global cognition in early  
578 Alzheimer's disease: A magnetic resonance imaging-electroencephalography study. *Brain*  
579 *Behav.* 2019;9(1):e01197.

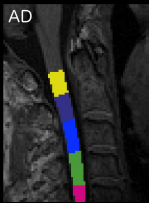
580 54. Amoroso N, La Rocca M, Bruno S, et al. Multiplex Networks for Early Diagnosis of  
581 Alzheimer's Disease. *Front. Aging Neurosci.* 2018;10:365.

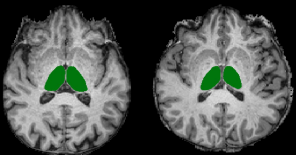
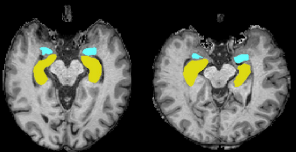
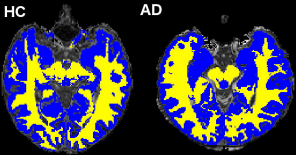
582

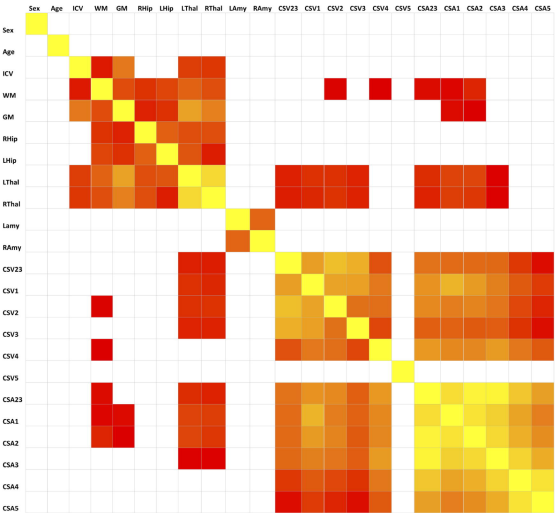
HC



AD







Predicted Class = AD

